


Article

Effect of Pouch Size on Sterilization of Ready-to-Eat (RTE) Bracken Ferns: Numerical Simulation and Texture Evaluation

Hwabin Jung ¹, Yun Ju Lee ¹ and Won Byong Yoon ^{1,2,*} 

¹ Department of Food Science and Biotechnology, College of Agriculture and Life Sciences, Kangwon National University, Chuncheon 24341, Republic of Korea

² Elderly-Friendly Food Research Center, Agriculture and Life Science Research Institute, Kangwon National University, Chuncheon 24341, Republic of Korea

* Correspondence: wbyoon@kangwon.ac.kr; Tel.: +82-33-250-6459

Abstract: Bracken fern (*Pteridium aquilium*, BF) is a widely consumed vegetable. It has the potential to be manufactured as a ready-to-eat (RTE) product as a cooking ingredient and a side dish. The aim of the current study was to develop sterilized BF RTE products and to investigate textural qualities depending on the size of the pouches. The F_0 -value at the cold point according to pouch size (100, 150, and 200 g) targeted at 15 min was determined through heat transfer simulation using the calibrated heat transfer coefficient. The location of the cold points in the stand-up pouches was moved upward from the bottom of the pouch by increasing the pouch size. The sterilization time for 100, 150, and 200 g was evaluated as 35.0, 41.5, and 47.5 min, respectively. The textural properties measured using the cutting test showed significant differences according to the location in the pouch. The textural degradation of BF in the top part of the pouch was more extensive than that at the bottom due to the smaller dimensions. In addition, the percentage of textural degradation in the top part increased with increasing pouch sizes. The methods introduced in this study can be applied to validate the degree of sterilization and the texture of various stalk vegetables used for ready-to-eat products packed in stand-up pouches.

Keywords: bracken fern; heat transfer simulation; home meal replacement; sterilization; texture of cooked vegetable



Citation: Jung, H.; Lee, Y.J.;

Yoon, W.B. Effect of Pouch Size on Sterilization of Ready-to-Eat (RTE) Bracken Ferns: Numerical Simulation and Texture Evaluation. *Processes*

2023, 11, 35. <https://doi.org/10.3390/pr11010035>

Academic Editors: Magdalena Kristiawan and Karim Allaf

Received: 24 October 2022

Revised: 16 December 2022

Accepted: 20 December 2022

Published: 23 December 2022



Copyright: © 2022 by the authors. Licensee MDPI, Basel, Switzerland. This article is an open access article distributed under the terms and conditions of the Creative Commons Attribution (CC BY) license (<https://creativecommons.org/licenses/by/4.0/>).

1. Introduction

In recent years, the home meal replacement (HMR) market, containing carbohydrates, proteins, and vegetables in a container, has attracted attention [1]. The demand for HMRS has been growing rapidly because of the increasing population of single households and consumers lacking time to cook [2]. Among HMR products, sterilized ready-to-eat (RTE) products for highly perishable vegetables are of interest in the food industry because they have a longer shelf-life while maintaining quality and meeting safety standards. Several retorted vegetable and vegetable side dishes using carrots, beans, roasted vegetables, and peas are already available. However, the development of other retorted vegetable products with acceptable quality and safety is needed.

The retort sterilization of vegetables to manufacture RTE products results in softening during heating [3]. Therefore, excessive heat treatment to inactivate spoilage microorganisms and pathogens is not desirable because the texture of vegetables is sensitive to thermal treatment. The sterilization process has to ensure adequate heat treatment to the “cold point”, a location with the slowest heating rate, during thermal processing, to reach sufficient sterility and minimize loss of product quality [4]. One of the important factors for the thermal process is the shape and size of the container holding the product. The container size for RTE products is diverse and depends on the number of servings. In terms of sterilization, the cold point of the product for each size must be determined before estimating the total thermal process. To investigate the temperature gradient during

thermal processes and find the cold point for RTE products with various sizes, numerical techniques for solving governing equations of heat transfer in a geometry have been used as practical tools [5]. The numerical solutions have successfully evaluated the cold point and estimated the degree of sterilization for the three-dimensional geometric analysis of food products with complicated shapes [6–9].

Bracken fern (*Pteridium aquilinum*, BF) is one of the most distributed plants in the world. BF species are used as a vegetable for food in Asia, mainly in China, Japan, and Korea [10]. After collecting young BF stalks, they are cooked, pickled, or dried for preservation. The major components of young BF are reported to be a high amount of protein (26.4%), sugars (19%), cellulose (12.5%), lignin (11.7%), pectic substances (5%), starch (2.75%), and hemicellulose [10]. In addition, BF has various biologically active compounds, such as polyphenols and flavonoids [11,12].

BF has the potential to be manufactured as an RTE product, which can be utilized as an ingredient for cooking or as a side dish after seasoning. However, when sterilizing stalk vegetables such as BF, it may be difficult to find the cold point. Moreover, when evaluating the texture of BF, there needs to be consideration for the geometry and shape because the shapes of the stalks are irregular. Therefore, this study aimed to develop BF RTE products with an adequate degree of sterilization and to investigate textural qualities depending on the size of the stand-up pouches. In the present study, the F_0 -value was calculated as a degree of sterilization at the cold point for various amounts of BF in pouches by conducting numerical simulations and evaluating the textural quality of sterilized BF according to the location in the pouch and the section of stalk using compression and cutting tests.

2. Materials and Methods

2.1. Sample Preparation

Dried young BF (*Pteridium aquilinum*) was purchased from a local market in Chuncheon, Republic of Korea. The moisture content of dried BF was $9.5 \pm 0.8\%$ (wet basis). Dried BF (100 g) was rinsed with distilled water to remove dust and blanched in 3 L of distilled water for 15 min. Afterward, the BF was soaked in distilled water for 3 h at room temperature. Water was drained after soaking, and the remained water on the surface of BF stalks was gently wiped using paper towels. Amounts of 100, 150, and 200 g of soaked BF were vacuum-packed in a retortable stand-up pouch (polyethylene terephthalate/low-density polyethylene) with a width of 16 cm and a height of 18 cm.

2.2. Numerical Simulation

The three different pouch geometries were used to simulate BF with the various amounts (100, 150, and 200 g) in the stand-up pouch. The governing equation of the three-dimensional transient heat transfer for conduction was the unsteady state Fourier's equation with an assumption of constant thermal diffusivity (α) [13]:

$$\frac{\partial T}{\partial t} = \alpha \nabla^2 T \quad (1)$$

where T is the temperature of the BF sample ($^{\circ}\text{C}$), t is the time (s), and α is the thermal diffusivity (m^2/s).

The surface conditions of the sample are:

$$-k \left(\frac{\partial T}{\partial x} \right) = -k \left(\frac{\partial T}{\partial y} \right) = -k \left(\frac{\partial T}{\partial z} \right) = h(T_s - T_{\infty}) \quad (2)$$

The sample has a uniform initial temperature; thus, the initial conditions are:

$$T(x, y, z, 0) = T_0 \quad (3)$$

The symmetry boundary conditions on the axes are:

$$\frac{\partial T}{\partial x} = \frac{\partial T}{\partial y} = \frac{\partial T}{\partial z} = 0 \quad (4)$$

From the above equations (Equations (2)–(4)): T_s is the temperature at the surface of the BF pouch ($^{\circ}\text{C}$), T_{∞} is the temperature of the steam in the retort, h is the heat transfer coefficient ($\text{W}/\text{m}^2\cdot\text{K}$), and k is the thermal conductivity ($\text{W}/\text{m}\cdot\text{K}$). The global heat transfer coefficient of the system is given by the sum of three thermal resistances in series. These are the convective resistances for bracken fern inside the pouch (h_i) and for the outer environment (h_o), and the conductive resistance of the package material layer. The latter is a function of the layer thickness and of the thermal conductivity. Therefore, the global heat transfer coefficient (h_g) in the system can be estimated as:

$$h_g = \left[\frac{1}{h_i} + \frac{L}{k} + \frac{1}{h_o} \right]^{-1} \quad (5)$$

where L is the thickness of the pouch material. Since the BF is vacuum packed in the pouch, the inside heat transfer coefficient (h_i) is eliminated. Therefore, the overall system is influenced by the heat transfer coefficient between the package material and the surrounding air. As the BF inside the pouch was assumed to be a continuum after vacuum-packed, the heat balance is:

$$mC_p \frac{\partial T}{\partial t} = -h_0 A (T_s - T_{\infty}) \quad (6)$$

where m is the mass of the bracken fern and A is the surface area of the pouch. Forced convection heat transfer is associated with fluid flow such as in retort operations that involve the generation of hot steam (air) to provide heat to the food product in a retort. The geometry under forced convection was assumed to be a horizontal plate for simplicity. However, this simplicity may give the heat transfer coefficient value, which is not ideal for reflecting the actual heat transfer in the pouch with an irregular shape compared to a plate. Therefore, calibration is required prior to the validation step based on the calculated heat transfer coefficient for a plate geometry. The heat transfer coefficient for a plate geometry is estimated from dimensionless numbers representing empirical correlations during the convective heat transfer:

$$Re = \frac{\rho u L}{\mu} \quad (7)$$

$$Pr = \frac{C_p \mu}{k} \quad (8)$$

for the laminar region,

$$Nu = 0.664 Re^{0.5} Pr^{\frac{1}{3}} \quad (9)$$

for the turbulent region,

$$Nu = 0.0366 Re^{0.8} Pr^{\frac{1}{3}} \quad (10)$$

$$h_0 = \frac{Nu k}{L} \quad (11)$$

where Re is Reynolds number, Pr is Prandtl number, Nu is Nusselt number, ρ is the density of air around the pouch, u is the flow speed, and μ is the dynamic viscosity of the air.

The constants in the above correlations are given in the literature [14] and are provided in Table 1. Thermal properties of BF, such as the thermal conductivity and specific heat, were measured using a KD2 Pro Thermal Properties Analyzer (Decagon Device, Pullman, WA, USA). The dual-needle thermal properties sensor was tightly fixed to the pouch, and BF was vacuum-packed. The BF pouch with the sensor was placed in a water bath and the thermal properties were measured every 10°C from 25 to 95°C . Each measurement was performed in triplicate, and the average value was used for the simulation. The density of

soaked BF at room temperature was measured using a basic volume method that measures weight in a container with a known volume [15]. The thermophysical properties of the retortable pouch were used for the heat transfer simulation in this study (Table 1).

Table 1. Thermal properties of soaked BF and the pouch.

| Property | Soaked BF | Pouch | Steam |
|---|--------------------|-------------------|---|
| Thermal conductivity (k) (W/m·K) | 0.26 ± 0.04 | 4.1 | |
| Specific heat (C_p) (J/kg·K) | 1209.9 ± 259.9 | - | $4 \times 10^{-5} T^2 - 0.004 T$ |
| Density (ρ) (kg/m ³) | 1490.2 ± 350.3 | - | $3 \times 10^{-6} T^3 - 0.0006 T^2 + 0.0408 T - 0.8059$ |
| Thickness (mm) | - | 0.15 | - |
| Dynamic viscosity (kJ/kg) | - | | $4 \times 10^{-8} T + 9 \times 10^{-6}$ |
| Source | - | Zhang et al. [16] | ThermExcel [14] |

Heat transfer simulation calculated using the finite volume method was performed using COMSOL version 5.3a Multiphysics software (COMSOL, Inc., Burlington, MA, USA). The size and shape of the pouches were determined based on the experimental measurements of packed BF. A mesh convergence study was performed by running the simulation with several different default mesh configurations of COMSOL, from “Coarser” to “Extremely fine” [17,18]. The results were considered to be independent of mesh resolution when the average temperature and the temperature at the cold point of the pouch between two sequential sets of meshes were less than 1% [19]. The mesh configuration was determined to be “Extra fine” due to the acceptable change. The detailed mesh convergence analysis, including the number of elements, maximum element size, and minimum element size, is shown in Table S1. Moreover, the adequacy of the mesh resolution was examined by calculating the grid convergence index (GCI), which shows a maximum of 1.51%, indicating mesh independence (Table S2). The detailed procedure to calculate GCI is exhibited in the supplementary [20]. The simulation was conducted at 30 s intervals to estimate the nodal temperature according to the results of the time-step dependence analysis (Table S3). The geometric design of the BF pouches is shown in Figure 1.

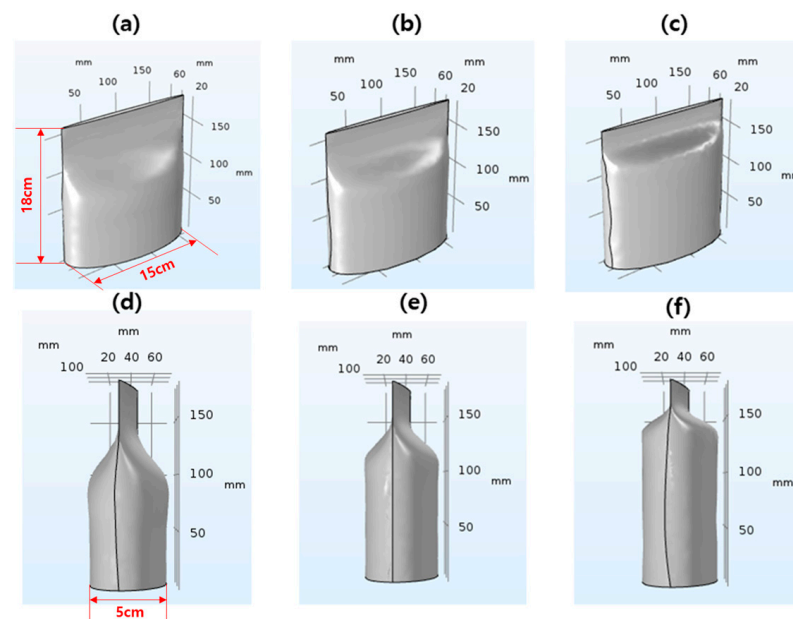


Figure 1. Geometric designs of vacuum-packed BF for simulation. Diagonal view of (a) 100 g, (b) 150 g, and (c) 200 g, and side view of (d) 100 g, (e) 150 g, and (f) 200 g pouches.

2.3. Sterilization Process

Sterilization was conducted using a retort sterilizer (SR-240, Tomy, Osaka, Japan). The temperature profiles of heating were recorded using a wireless thermocouple (Tracksense[®] pro, Ellab, Hilleroed, Denmark) during heating from 18 °C to 121.1 °C for 90 min. The wireless thermocouple was also located at the cold point of the BF samples obtained by numerical simulation. The F_0 -value was targeted to 15 min for solar-dried vegetable products with high initial microorganisms to achieve six months of shelf life at room temperature (Korean patent No. KR20200125370A).

2.4. F-Value Calculation

The F -value, which represents the degree of sterilization, was calculated where a reference temperature of 121.1 °C and a z -value of 10 °C were applied based on the sterilization conditions for thermoresistant anaerobic *Clostridium botulinum* spores [21].

$$F = \int_{t_0}^{t_f} 10^{\frac{T_c - T_{ref}}{z}} dt \quad (12)$$

where t_0 is the initial heating time (min), t_f is the final heating time (min), T_c is the temperature at the cold point (°C), T_{ref} is the reference temperature (°C), and F is the lethality or sterilization value (min). The values of t_0 and T_{ref} in this study are 0 min and 121.1 °C, respectively.

2.5. Textural Measurements

The textural characteristic of BF stalks was measured using two methods, the compression and cutting tests. Force–displacement curves were obtained by recording the detected force during the texture probe compress or by cutting the BF in time series using a texture analyzer (TA-XT plus 100 Connect, Stable Micro Systems, Surrey, UK). The displacement was converted using a test speed (0.5 mm/s). The measurement of sterilized BF was conducted at three different segments of the stalk based on the normalized length: lower stipe (I, 0 to 0.3), upper stipe (II, 0.3 to 0.7), and fiddlehead (III, 0.85 to 1.0) (Figure 2a). BF was also sampled at three locations, having an equal length from the bottom to the top of the pouched BF after sterilization: top (T), middle (M), and bottom (B) (Figure 2b). For the compression test, the BF at each segment was cut into lengths of 10 mm, then measured using a cylindrical probe (38.1 mm diameter) with 50% deformation, 0.5 mm/s crosshead speed, and 2 g trigger force. The average diameter of each segment was measured for 300 BF stalks using a vernier caliper, and it was 0.85 ± 0.08 , 0.51 ± 0.11 , and 0.15 ± 0.08 cm for lower stipe, upper stipe, and fiddlehead, respectively. The true stress of the BF was calculated using the following equation:

$$\text{True stress (g/mm}^2\text{)} = \frac{F_1}{L \times d} \quad (13)$$

where F_1 is the compression force, L is the length of the segment (10 mm), and d is the diameter.

The cutting force was obtained by shear curves using a thin blade probe (0.3 mm of thickness) at a crosshead speed of 0.5 mm/s. The measurement was carried out at several locations in each segment. The shear stress was calculated as:

$$\text{Shear stress (g/mm}^2\text{)} = \frac{F_2}{t \times d} \quad (14)$$

where F_2 is the cutting force, and t is the thickness of the blade probe (0.3 mm).

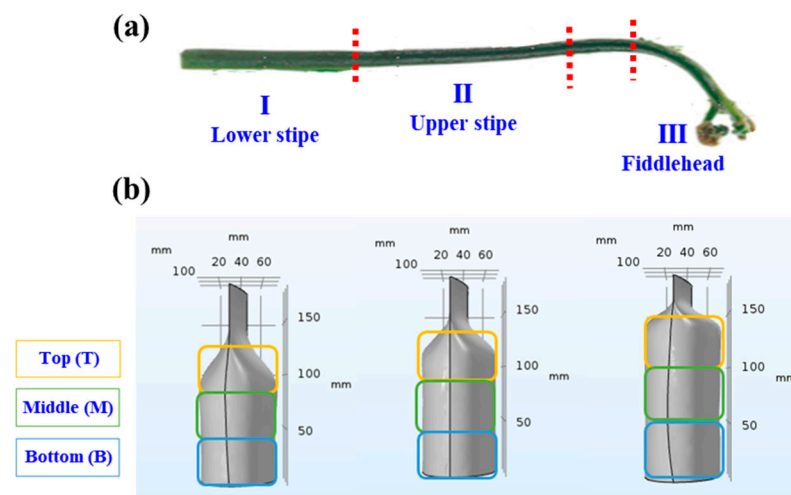


Figure 2. The sampling locations for textural measurements of sterilized BF. (a) Segment location on a BF stalk and (b) sampling location in a stand-up pouch. The red dashed line is to distinguish the section.

2.6. Statistical Analysis

The simulated data were validated using experimental data (temperature and F -value), and the following equations were used to calculate the root mean squared error (RMSE):

$$\text{RMSE}_{\text{Temp}} = \sqrt{\frac{\sum_{i=0}^n (T_e - T_s)^2}{n}} \quad (15)$$

$$\text{RMSE}_{F\text{-value}} = \sqrt{\frac{\sum_{i=0}^n (F_e - F_s)^2}{n}} \quad (16)$$

where T_e is the sample temperature measured in the experiment, T_s is the simulated temperature, F_e is the F -value calculated using the experimental temperature, F_s is the F -value calculated using the simulated temperature, and n is the number of data points. Significant differences were evaluated through one-way analysis of variance (ANOVA) using MS-Excel 2016 (Microsoft, Redmond, WA, USA) at a confidence level of 95%.

3. Results and Discussion

3.1. Numerical Simulation for the Cold Point in Stand-Up Pouches

Heat transfer simulation was performed to find the cold point of BF packed in a stand-up pouch for three different amounts of sample. The results of the heat transfer simulation for the BF pouches are shown in Figure 3. From the temperature distribution, the cold point was found to be at the location from the bottom-center of the pouch, 4.3, 6.6, and 7.8 cm for the 100, 150, and 200 g BF pouches, respectively. The location of the cold point increased with increases in the amount of the sample, but the location of the cold point was not linearly proportional to the amount of BF ($R^2 < 0.97$). The vertical diversity in the length of the pouches that contained BF possibly caused a random change in the location of the cold point. The heat transfer simulation is useful for finding the cold point in a complex geometric vessel such as the pouches in this work. Lee and Yoon [22] reported an investigation of the transient location of the slowest heating zone during the sterilization of liquid food in a can. In a study by Hong et al. [23], heat transfer simulation was used to predict the cold point of pasteurized carrots packed in various sizes and geometries.

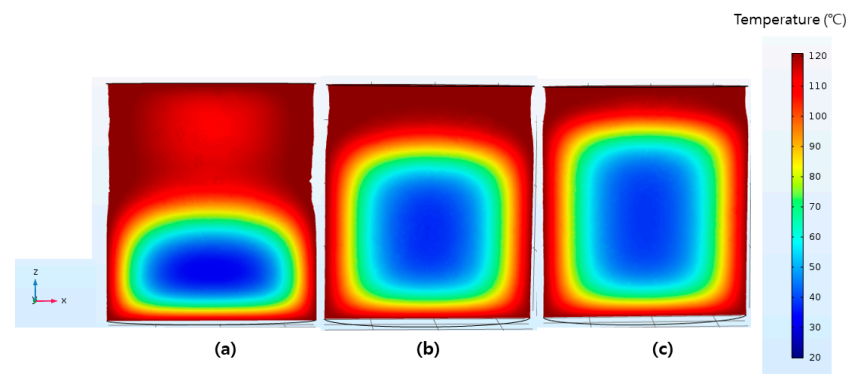


Figure 3. Simulated temperature distribution resulting from heat transfer simulation in BF samples of different amounts of (a) 100 g, (b) 150 g, and (c) 200 g in stand-up pouches.

In accordance with the simulation for the location of the cold point, the temperature profiles of three different amounts of packed BF were measured at the cold point during sterilization at 121.1 °C (Figure 4). In addition, the location of the cold point was validated by measuring temperature at different heights of the sample using four-logger wireless temperature sensor (data not shown). The initial h analytically calculated by Equations (7)–(11) was 251.4 W/m²·K based on the thickness of the bottom-center of the pouch. Biot number was 18.4, indicating a temperature gradient in the sample during thermal processing. The h was calibrated to determine the optimum value, which shows the low RMSE, since the shape was assumed to be a plate for simplicity. The average thickness must be smaller than 5 cm due to the shape of the standing pouch; thus, simulation was conducted using the h value ranging from 251.4 to 350 W/m²·K (Figure 4).

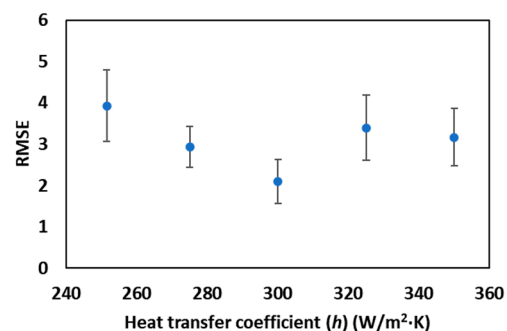


Figure 4. Average RMSE for three BF samples with different amounts of BF in the pouch depending on h .

The most appropriate value of h which shows a low average RMSE for sterilized BF in various pouch sizes was 300 W/m²·K (<2.1 °C); thus, it was used to perform further simulations. The results presented in Figure 5 show that temperature profiles from the heat transfer simulation obtained using the calibrated heat transfer coefficient fit the temperature profiles from the experiments well. When the size of the packed BF was increased by increasing the amount of the sample, the temperature at the cold point increased at a slower rate. In addition, the time at which the temperature began to increase in the sample using thermal treatment was longer for larger pouches. Consequently, those larger pouches reached an equilibrium temperature more slowly than smaller pouches. The heating rates for each pouch size were distinct, even though the length (i.e., the dimension in the y -direction) at the cold point was nearly identical. This is due to an insufficient increase in the surface area whilst the amount of sample increased. A significant relationship between volume and surface area of the packed vegetable upon sterilization was reported in a study of Hong et al. [23]. The lag time for increasing temperature was possibly due to the low thermal conductivity of BF. It is interesting to note that the temperature of the 200 g pouch was increased faster compared to the other samples (Figure 5). The shape of the 200 g

pouch was closer to that of a slab, and this resulted in the short time to reach temperature of the heating medium. This result is in agreement with a study by Park and Yoon [6], which reported that randomly packed rice cakes with an oval shape showed a slower heating rate and a long come-up time. In contrast, a rapid increase in temperature was observed for the same amount of rice cake in a slab-shaped pouch. The packed BF was considered a continuous solid medium in the simulation of this study, and the simplification successfully described heat transfer into the clump of a stalk vegetable.

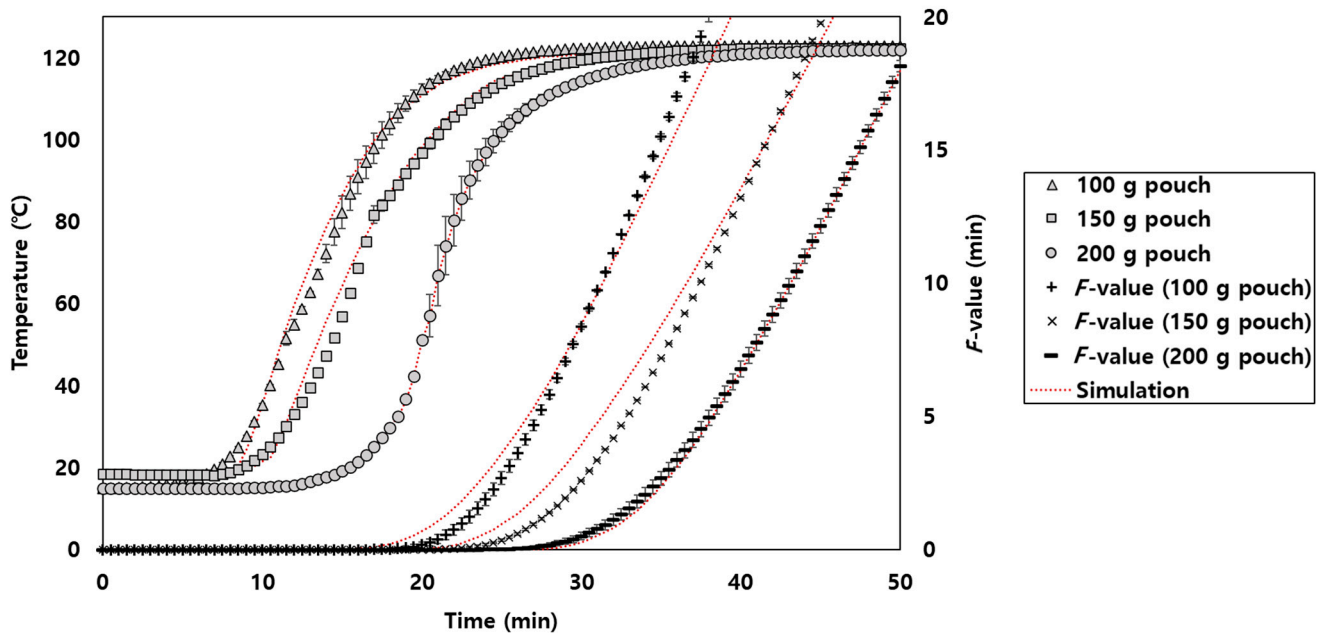


Figure 5. Temperature profile at the cold point obtained experimentally and by simulation and the calculated F -values for packed BF at amounts of 100, 150, and 200 g.

3.2. Calculation of F -Value

The F -value at the cold point of BF packed in various amounts was calculated based on the temperature profiles obtained both experimentally and by simulation (Figure 5). The retort sterilization time for F_0 -value = 15 min for BF was 35.0, 41.5, and 47.5 min for 100, 150, and 200 g pouches, respectively. In addition, the RMSE of the F_0 -value was 1.73, 0.73, and 0.12 min for 100, 150, and 200 g pouches, respectively, indicating a good correlation with the simulation. The higher RMSE for the smaller sample size was considered to be due to the higher rate of heat penetration affected by the wireless thermocouple embedded in the sample, which has high thermal conductivity [23]. The longer sterilization time for BF due to the high F_0 likely influenced the textural properties of the sample. In particular, a pouch with non-uniform thickness can cause textural variations in the BF in the pouch through changes in thermal treatment time. Similar to the long-time retort processing of this study, the same crucial problem has been reported for the sous-vide processing of vacuum-packed food products about the non-uniform cooking effect within large products [24].

3.3. Texture Softening of BF after Sterilization

Texture measurement of sterilized BF was conducted to evaluate the uniformity depending on the amount of BF, which is highly related to overall quality. The most pronounced texture of cooked BF is considered to be toughness related to sensory property. In the study of Rodrigues-Arcos et al. [25], the toughness of green asparagus was evaluated using a cutting test because the force required to cut the spear is correlated with fibrousness. In addition, a compression test was conducted to measure internal failure, which is the least localized test among the texture measurement methods for stem sections of asparagus. Therefore, a compression test on each stalk section of BF was carried out to obtain information about structural change by thermal treatment. The results of the textural measurements

of sterilized BF according to the segment of the stalk and the location in the pouches are shown in Tables 2 and 3. In a comparison of the compression and cutting tests, the cutting test results better characterized the differences in each segment and location in the pouch. For all segments of the BF stalk, longer heating times with increased amounts inside the pouch decreased stress. In addition, the location of the BF inside the pouch significantly contributed to the textural variations. The least stress change was observed at the middle part of the pouch where the cold point existed. In contrast, the most significant change in the top part of the pouch represented the excessive heating of BF in the thinner top part. The stress of the fiddlehead (III) part in the compression test was relatively consistent with the other parts, whereas softening was detected in the cutting test. This might have been due to the structure of the fiddlehead, which is curled at the crozier stage that forms a soft young leaf when it is uncurled. The texture of BF is anticipated to soften through thermal processing at temperatures above 80 °C as do those of other vegetables, such as carrots [26], potatoes [27], and celery [28]. The textural softening of BF was due to depolymerization of the pectic galacturonan chain by β -eliminative degradation by heating [29,30]. The texture of BF might maintain a moderate toughness despite excessive thermal treatment because part of the cellulose fraction of BF does not undergo thermal degradation using heat treatment. However, it is necessary to modify the shape or size of the pouch for the larger sizes to achieve the uniform quality of the product. Similar to this result, a study about the effect of orientation of the bottled liquid food on quality after sterilization showed that the shorter the thermal processing time was, the more the chance of retaining the final quality of the product increased [31].

Table 2. True stress (kPa) measured using the compression test of sterilized BF. T, M, and B correspond to the top, middle, and bottom, respectively, in Figure 2b for the sampling location in a stand-up pouch.

| Amount | True Stress (kPa) | | | | | | | | |
|--------|-------------------|--------------|---------------|--------------|--------------|---------------|--------------|--------------|--------------|
| | 100 g | | | 150 g | | | 200 g | | |
| | Part | I | II | III | I | II | III | I | II |
| T | 448.2 ± 67.2 | 380.4 ± 54.8 | 300.5 ± 88.9 | 400.5 ± 54.1 | 304.7 ± 80.9 | 276.3 ± 346.4 | 301.5 ± 61.5 | 250.8 ± 60.7 | 200.1 ± 60.7 |
| M | 480.5 ± 84.3 | 420.8 ± 68.5 | 380.94 ± 68.5 | 467.9 ± 96.6 | 387.0 ± 73.6 | 310.8 ± 60.5 | 420.4 ± 73.0 | 372.0 ± 50.1 | 300.9 ± 50.1 |
| B | 467.6 ± 59.6 | 402.0 ± 40.0 | 348.12 ± 66.9 | 438.8 ± 87.3 | 354.9 ± 69.7 | 307.8 ± 60.8 | 380.9 ± 69.7 | 357.9 ± 47.4 | 295.5 ± 47.4 |

Table 3. Shear stress (kPa) measured by the cutting test of sterilized BF. T, M, and B correspond to the top, middle, and bottom, respectively, in Figure 2b for the sampling location in a stand-up pouch.

| Amount | Shear Stress (kPa) | | | | | | | | |
|--------|--------------------|-----------|-----------|-----------|-----------|-----------|-----------|-----------|-----------|
| | 100 g | | | 150 g | | | 200 g | | |
| | Part | I | II | III | I | II | III | I | II |
| T | 2.2 ± 0.3 | 1.1 ± 0.2 | 0.4 ± 0.4 | 2.0 ± 0.4 | 0.9 ± 0.3 | 0.5 ± 0.2 | 1.3 ± 0.1 | 0.4 ± 0.1 | 0.3 ± 0.1 |
| M | 2.5 ± 1.0 | 1.2 ± 0.3 | 0.5 ± 0.2 | 2.4 ± 0.9 | 1.2 ± 0.3 | 0.7 ± 0.2 | 2.3 ± 0.9 | 1.1 ± 0.3 | 0.6 ± 0.2 |
| B | 2.2 ± 0.1 | 1.1 ± 0.4 | 0.5 ± 0.3 | 2.0 ± 0.3 | 1.1 ± 0.3 | 0.6 ± 0.2 | 1.9 ± 0.5 | 0.9 ± 0.2 | 0.5 ± 0.4 |

4. Conclusions

Textural changes according to the amount (100, 150, and 200 g) of sterilized BF were investigated based on the stalk segment and BF location in the pouch. The cold point of BF packed in a stand-up pouch was well-predicted using heat transfer simulation. The simulated temperature profiles at the cold point using the calibrated heat transfer coefficient and the experimental results were well-fitted. When the size of the pouch of BF was increased, the distance from the bottom to the cold point was increased. In addition, the heating time to reach the F_0 -value was increased with increasing sizes of the pouch. When the amount of BF was doubled from 100 to 200 g, sterilization time at the cold point was increased from 35 to 47.5 min, which is not proportional to the amount of sample in the

pouch. The shape of the pouch affects the location of the cold point and the temperature increase rate at the cold point. The measurement method to analyze texture according to the segment of the stalk and the location of BF in the pouch was estimated using the cutting test. With respect to the location of BF in the pouch, the degree of textural degradation was high in the order of top, bottom, and middle. The highest textural degradation was in the top part, at 61%. In addition, the ratio of textural degradation was increased with increasing sizes of the pouch. Textural quality related to uniformity is difficult to achieve even though the sterilization time was optimized to avoid the excessive heat. Therefore, it is required to modify the shape or enlarge the pouch size of the BF to achieve uniform quality by shortening sterilization time. Thus, numerical simulation plays an important role as a tool to find the cold point and to optimize sterilization time by calculating *F*-value. Moreover, the thermal properties can be used to design the scaled-up product and optimize the sterilization process for various sizes of products within the industry. This study demonstrated that heat transfer simulation and textural measurements according to the amount of BF in the container was useful to describe the temperature profiles at the cold point, and the method of evaluating the textural properties of the BF product could be applied to other types of stalk vegetables used in RTE foods. In addition, designing simple numerical simulations, including calibrating the heat transfer coefficient in this study, is suggestive of thermal sterilization of vacuum-packed food products.

Supplementary Materials: The following supporting information can be downloaded at: <https://www.mdpi.com/article/10.3390/pr11010035/s1>, Table S1. Effect of mesh resolution on the average temperature and the cold point temperature of BF pouch. Table S2. Calculations of values using Equations (S1)–(S6). Table S3. Effect of time-step on the average temperature and the cold point temperature of BF pouch.

Author Contributions: Conceptualization, H.J., Y.J.L. and W.B.Y.; methodology, Y.J.L. and W.B.Y.; software, Y.J.L.; validation, Y.J.L.; investigation, H.J., Y.J.L. and W.B.Y.; writing—original draft preparation, Y.J.L. and W.B.Y.; writing—review and editing, H.J. and W.B.Y.; supervision, W.B.Y. All authors have read and agreed to the published version of the manuscript.

Funding: Following are results of a study on the “Leaders in Industry-university Cooperation 3.0” Project [202212050001], supported by the Ministry of Education and National Research Foundation of Korea. This research was supported by the Basic Science Research Program through the National Research Foundation of Korea (NRF), funded by the Ministry of Education (NRF-2018R1D1A3B06042501).

Institutional Review Board Statement: Not applicable.

Informed Consent Statement: Not applicable.

Data Availability Statement: The data presented in this study are available on request from the corresponding author.

Conflicts of Interest: The authors declare no conflict of interest.

References

1. Costa, A.I.A.; Dekker, M.; Beumer, R.R.; Rombouts, F.M.; Jongen, W.M. A consumer-oriented classification system for home meal replacements. *Food Qual. Prefer.* **2001**, *12*, 229–242. [[CrossRef](#)]
2. Bumbudsanpharoke, N.; Ko, S. Packaging technology for home meal replacement: Innovations and future prospective. *Food Control* **2022**, *132*, 108470. [[CrossRef](#)]
3. Yuan, L.; Xu, F.; Xu, Y.; Wu, J.; Lao, F. Production of marinated Chinese lotus root slices using high-pressure processing as an alternative to traditional thermal-and-soaking procedure. *Molecules* **2022**, *27*, 6506. [[CrossRef](#)] [[PubMed](#)]
4. Park, H.W.; Yoon, W.B. Computational fluid dynamics (CFD) modelling and application for sterilization of foods: A review. *Processes* **2018**, *6*, 62. [[CrossRef](#)]
5. Alias, N.; Satam, N.; Darwis, R.; Hamzah, N.; Ghaffar, Z.S.A. Some parallel numerical methods in solving partial differential equations. In Proceedings of the 2nd International Conference on Computer Engineering and Technology, Chengdu, China, 16–18 April 2010.
6. Park, H.W.; Yoon, W.B. A quantitative microbiological exposure assessment model for *Bacillus cereus* in pasteurized rice cakes using computational fluid dynamics and Monte Carlo simulation. *Food Res. Int.* **2019**, *125*, 108562. [[CrossRef](#)]

7. Dimou, A.; Stoforos, N.G.; Yanniotis, S. Effect of particle orientation during thermal processing of canned peach halves: A CFD simulation. *Foods* **2014**, *3*, 304–317. [CrossRef]
8. Jahanbakhshian, N.; Hamdami, N. Numerical simulation of heat and mass transfer during heating and cooling parts of canned-green-olive pasteurization. *J. Food Process Eng.* **2021**, *44*, e13909. [CrossRef]
9. Azar, A.B.; Ramezan, Y.; Khashehchi, M. Numerical simulation of conductive heat transfer in canned celery stew and retort program adjustment by computational fluid dynamics (CFD). *Int. J. Food Eng.* **2020**, *16*, 20190303. [CrossRef]
10. Kreshchenok, I.; Lesik, E.; Tousehkin, A.; Tousehkina, A. Edible ferns of the amur region and their rational use. *IOP Conf. Ser. Earth Environ. Sci.* **2021**, *937*, 022138. [CrossRef]
11. Fukuoka, M.; Kuroyanagi, M.; Yoshihira, K.; Natori, S. Chemical and toxicological studies on bracken fern, *Pteridium aquilinum* var. *latiusculum*. II. Structures of pterosins, sesquiterpenes having 1-indanone skeleton. *Chem. Pharm. Bull.* **1978**, *26*, 2365–2385. [CrossRef]
12. Park, C.; Kim, K.; Yook, H. Comparison of antioxidant and antimicrobial activities of bracken (*Pteridium aquilinum* Kuhn) according to cooking methods. *Korean J. Food Nutr.* **2014**, *27*, 348–357. [CrossRef]
13. Ishiwatari, N.; Fukuoka, M.; Sakai, N. Effect of protein denaturation degree on texture and water state of cooked meat. *J. Food Eng.* **2013**, *117*, 361–369. [CrossRef]
14. Steam Characteristics (from 0 to 30 bar); Therm Excel. 2003. Available online: https://www.thermexcel.com/english/tables/vap_eau.htm (accessed on 20 October 2022).
15. Huang, Z.; Zhu, H.; Yan, R.; Wang, S. Simulation and prediction of radio frequency heating in dry soybeans. *Biosyst. Eng.* **2015**, *129*, 34–47. [CrossRef]
16. Zhang, H.; Bhunia, K.; Munoz, N.; Li, L.; Dolgovskij, M.; Rasco, B.; Tang, J.; Sablani, S.S. Linking morphology changes to barrier properties of polymeric packaging for microwave-assisted thermal sterilized food. *J. Appl. Polym. Sci.* **2017**, *134*, 45481. [CrossRef]
17. Alfaihi, B.; Tang, J.; Jiao, Y.; Wang, S.; Rasco, B.; Jiao, S.; Sablani, S. Radio frequency disinfection treatments for dried fruit: Model development and validation. *J. Food Eng.* **2014**, *120*, 268–276. [CrossRef]
18. Goñi, S.M.; d'Amore, M.; Della Valle, M.; Olivera, D.F.; Salvadori, V.O.; Marra, F. Effect of load spatial configuration on the heating of chicken meat assisted by radio frequency at 40.68 MHz. *Foods* **2022**, *11*, 1096. [CrossRef] [PubMed]
19. Moradi, M.; Rashedi, H.; Mofradnia, S.R.; Khosravi-Darani, K.; Ashouri, R.; Yazdian, F. Polyhydroxybutyrate production from natural gas in a bubble column bioreactor: Simulation using COMSOL. *Bioengineering* **2019**, *6*, 84. [CrossRef]
20. Celik, I.B.; Ghia, U.; Roache, P.J.; Freitas, C.J. Procedure for estimation and reporting of uncertainty due to discretization in CFD applications. *J. Fluids Eng.* **2008**, *130*, 078001. [CrossRef]
21. Smout, C.; Van Loey, A.; Hendrickx, M. Non-uniformity of lethality in retort processes based on heat distribution and heat penetration data. *J. Food Eng.* **2000**, *45*, 103–110. [CrossRef]
22. Lee, M.G.; Yoon, W.B. Developing an effective method to determine the deviation of F value upon the location of a still can during convection heating using CFD and subzones. *J. Food Process Eng.* **2014**, *37*, 493–505. [CrossRef]
23. Hong, Y.; Uhm, J.; Yoon, W.B. Using numerical analysis to develop and evaluate the method of high temperature Sous-Vide to soften carrot texture in different-sized packages. *J. Food Sci.* **2014**, *79*, E546–E561. [CrossRef] [PubMed]
24. Onyeaka, H.; Nwaizu, C.C.; Ekaette, I. Mathematical modeling for thermally treated vacuum-packaged foods: A review on sous vide processing. *Trends Food Sci. Technol.* **2022**, *126*, 73–85. [CrossRef]
25. Rodriguez-Arcos, R.C.; Smith, A.C.; Waldron, K.W. Mechanical properties of green asparagus. *J. Sci. Food Agric.* **2002**, *82*, 293–300. [CrossRef]
26. Peng, J.; Tang, J.; Barrett, D.M.; Sablani, S.S.; Powers, J.R. Kinetics of carrot texture degradation under pasteurization conditions. *J. Food Eng.* **2014**, *122*, 84–91. [CrossRef]
27. Moyano, P.C.; Troncoso, E.; Pedreschi, F. Modeling texture kinetics during thermal processing of potato products. *J. Food Sci.* **2007**, *72*, E102–E107. [CrossRef]
28. Zor, M.; Sengul, M.; Karakütük, İ.A.; Odunkiran, A. Changes caused by different cooking methods in some physicochemical properties, antioxidant activity, and mineral composition of various vegetables. *J. Food Process. Preserv.* **2022**, *46*, e16960. [CrossRef]
29. Van Buren, J.P.; Kean, W.P.; Gavitt, B.K.; Sajjaanantakul, T. Effects of salts and pH on heating-related softening of snap beans. *J. Food Sci.* **1990**, *55*, 1312–1314. [CrossRef]

30. Gong, C.; Zhao, Y.; Zhang, H.; Yue, J.; Miao, Y.; Jiao, S. Investigation of radio frequency heating as a dry-blanching method for carrot cubes. *J. Food Eng.* **2019**, *245*, 53–56. [[CrossRef](#)]
31. Lespinard, A.R.; Badin, E.E.; Santos, M.V.; Mascheroni, R.H. Computational fluid dynamics analysis on natural convective heating of bottled liquid food during pasteurization: Effect of container orientation. *J. Food Process Eng.* **2019**, *42*, e12995. [[CrossRef](#)]

Disclaimer/Publisher's Note: The statements, opinions and data contained in all publications are solely those of the individual author(s) and contributor(s) and not of MDPI and/or the editor(s). MDPI and/or the editor(s) disclaim responsibility for any injury to people or property resulting from any ideas, methods, instructions or products referred to in the content.